

ITU-R Path Loss Model of Semi-Arid Region

Maddikera Krishna Reddy, Banreddy Likhitha, Pinjari Shakila, Shaik Sana Sultana, Challa Vanitha, Dadi Sravani

Cite as: Reddy, M. K., Likhitha, B., Shakila, P., Sultana, S. S., Vanitha, C., & Sravani, D. (2024). ITU-R Path Loss Model of Semi-Arid Region. International Journal of Microsystems and IoT, 2(11), 1356–1361. <https://doi.org/10.5281/zenodo.15063182>



© 2024 The Author(s). Published by Indian Society for VLSI Education, Ranchi, India



Published online: 29 November 2024



Submit your article to this journal:



Article views:



View related articles:



View Crossmark data:



DOI: <https://doi.org/10.5281/zenodo.15063182>

Full Terms & Conditions of access and use can be found at <https://ijmit.org/mission.php>



ITU-R Path Loss Model of Semi-Arid Region

Maddikera Krishna Reddy, Banreddy Likhitha, Pinjari Shakila, Shaik Sana Sultana, Challa Vanitha, Dadi Sravani

Electronics and Communication Engineering, G.Pullaiah College of Engineering and Technology, Kurnool, India

*Corresponding Author (krishnareddymaddikeras@gmail.com)

ABSTRACT

Rainfall fade slope is an important factor that system engineers consider when developing fading mitigation procedures (FMT) for microwave systems in space-earth situations measures the rate at which rain attenuates radio signals. The accuracy with which the ITU-R's suggested fade slope prediction model approximates the distribution of fade slopes within tropical regions has been confirmed by a recent analysis conducted in Kurnool, India. The entire year-long measurement effort yielded results that are in good agreement with empirical data. Furthermore, the findings were validated by a meticulous cross-referencing of the information collected for this study with rainfall records in hierarchical data format (HDF view) obtained from NASA's HDF view.

KEYWORDS

Tropical region, ITU-R model, rain fade slope, path loss and fade durations.

1. INTRODUCTION

The ability to send millimetre waves across short distances efficiently is critical to the future of wireless communication. Nevertheless, employing millimetre-wave spectral areas poses signal transmission issues in contrast to the sub-6 GHz frequency range. Among them are multipath fading, multipath delay spread, multipath loss, and shadowing. Furthermore, the propagation channel characteristics vary depending on whether the environment is indoors or outdoors, which has a significant impact on the dependability of critical metrics in physical layer design such as outage probability, packet error rate (PER), signal-bit error rate (BER), interference plus noise ratio (SINR), and symbol error rate (SER). Understanding these variations is crucial for optimizing the performance of wireless communication systems in different scenarios. It allows for the development of more accurate models and algorithms to improve overall system reliability and efficiency [2].

Path Loss Calculation:

Path loss models are crucial for rural areas, especially for transmitters above 35 meters, as they predict signal strength and interference. In outdoor microcellular channels, these models are generally independent of frequency. However, frequency dependence is present during the first meter of propagation loss and operates on the square of the frequency. Throughout the mm-wave spectrum, frequency dependency is also seen in rain and oxygen absorption. Directional antennas introduce additional distance dependent path loss compared to omni directional antennas, as they function as spatial filters, missing multipath energy from non-targeted directions.

In order to prevent overestimating interference or coverage, researchers should proceed with caution and refrain from using directional antenna gains in route loss models intended for omni directional formulations. The 3GPP RMa LOS path loss model serves as a tool for statistically modelling path loss over distance, specifically for clear, unobstructed paths between transmitters and receivers [3].

$$PL_1[\text{dB}] = 20 \log_{10}(40\pi \cdot d3D \cdot f_c/3) \quad (1)$$

The well-known Friis equation (Friis, 1946) governs radio propagation in free space:

$$P_r = P_t (G_r G_t \lambda^2 / 4\pi d) \quad (2)$$

Where, P_r , P_t stands for the power at the transmitter and receiver, respectively; G_r , G_t stands for the corresponding antenna gains; λ stands for the radiation wavelength; and d stands for the distance between the transmitter and receiver. 'Path loss' (PL), which is defined as $PL = 10 \log P_t/P_r$, is a common way to represent power attenuation. In light of this, the route loss in space may be stated as

$$PL_{\text{Free-space}} = -27.56 + 20 \log_{10}(f) + 20 \log_{10}(d) \quad (3)$$

2. LITERATURE REVIEW

2.1 Path loss Review

At a distance of 20 km, the route loss for the TV terrestrial transmitter at Kota Padang was determined using the ITU-R P.1546-5 technique. Pemancar ANTV at 663.25 MHz had the lowest path loss of all the transmitters, whereas Pemancar Indusial at 695.25 MHz had the most.

When using TV penance frequency, the ITU.R. P.1546-5 approach for route loss permutation produced non-linear results. The antenna was extremely sensitive to route loss. The ITU-R P.525-2 approach is not as accurate as this one. It is twenty kilometers from the nearest TV transmitter.[4] The substantial distance way misfortune model asserts that the usual signal effect in radio channels reduces logarithmically with distance, expressing this principle as follows:

$$PL(d) \propto (d/d_0)^n \quad (4)$$

$$PL(\text{dB}) = PL(d_0) + 10n \log(d/d_0). \quad (5)$$

ITU-R P.1546-3, Hata, Davidson, COST 231, ITU-R P.5293, CCIR, ECC, Egli, WI, and other path loss prediction models are used in the study to estimate path loss along preset routes, and their accuracy is compared with real measurements. Metrics including mean error, prediction error distribution, spread corrected root mean square error (SC-RMSE), and root mean square error (RMSE) are used in the study's evaluation of route loss prediction models. Better performance is shown by lower RMSE values, whereas SC-RMSE accounts for error dispersion spread. For every model, the prediction error distribution is examined and the mean error between the measured and anticipated route loss values is found [5]. The "model A" (UMi_A) and "model B" (UMi_B) versions of route loss modeling, which span 4G and 5G urban microcell scenarios, are the main emphasis of this study. UMi_A covers the frequencies between 0.5 and 6 GHz, whereas UMi_B covers the bands between 0.5 and 100 GHz. Three important frequency bands—2.6 GHz, 3.5 GHz, and 5.62 GHz—which correlate to the 5G n7, n78, and n46 operating bands—are compared in this study. Users are anticipated to be in line-of-sight (LOS) with the base station (BS) antenna in the UMi_A cell situations. In the UMi_A cell scenarios, a 20 MHz bandwidth is available at each tier. The frequency range determines the transmitter power at the micro cell: Between 2.6 and 3.5 GHz and 5.62 GHz, 40 dBm is available [6]. Anritsu MS2712E Spectrum Master and a digital RF signal generator were used in a study's signal transmission and reception tests at the Veritas Hall C building in South Korea. There were cement mortar barriers in the direct line of sight for both the transmission and the receiving. A 20 dBm transmission power setting was used. The number of barriers rose linearly with the route loss they introduced. The empirically observed path loss per wall was 17.78 dB, while the experimentally estimated path-loss exponent was 3 [7].

3. METHODOLOGY

Rainfall rate and rain rate are all taken into consideration in NASA Earth data, which includes a variety of data kinds and locations. In this case, we consider the location of Andhra Pradesh, Kurnool, India, as indicated in Fig 1.

In this work, a step-by-step technique and approach for analyzing route loss are presented below:

Step1: To begin analysis and graphing, all the data gathered from the NASA Earth data base are arranged and entered into Matlab. depicts the flow chart used in research to calculate path loss based on collected data.

Step 2: Analyze the phenomenon of path loss at 38 GHz across a 0.03 km path length in rainy air. Figure 1 displays the free space propagation loss, atmospheric gasses, shadowing, rain fade slope, rain fade length, and rain rate for Kurnool, Andhra Pradesh, India, which is located at 15.8°N and 78.0°E.

Step 3: Notable discoveries include average path losses, the highest amount of PL that can be found during the day, and records of the slope at which rain falls in relation to the rain rate.

Step 4: Provide the optimal recommendation for a PL model across a brief route at millimeter-wave.

Step 5: A detailed description of the LOS parameter analysis may be found in the next section.



Fig. 1 Location of Kurnool, Andhra Pradesh, India with climate change

$$LLoS = L_0 + 10n \log_{10}(d/1000) + A_{\text{gas}} + A_r \quad (6)$$

Parameter of the path loss:

$$PL_{\text{dB}} = \beta LLoS + 10\gamma \log_{10}(f_{\text{GHz}}) + 10\alpha \log_{10}(d/1) + x\sigma \quad (7)$$

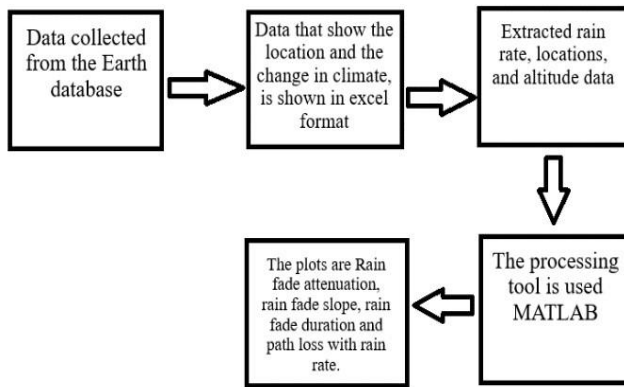


Fig. 2 Data Processing

A. Path Loss method:

Course loss in wi-fi communication structures is calculated with the usage of the following equations, and it's far laid low with several variables and factors. allow us to deconstruct these equations, have a look at their effects, and conclude:

Line of Sight Loss (L_{LoS}) Calculation:

$$L_0 + 10\log_{10}(d/1000) + A_{gas} + A_r \quad (8)$$

The primary machine is supposed to compute line of sight loss (L_{LoS}) by way of combining several essential elements:

L_0 represents the sign depth loss for the duration of a onekilometer distance in an open area. The expression $10\log_{10}(d/\text{one thousand})$ considers course loss because of the distance between transmitter and receiver, wherein 'n' represents the course loss exponent. A_{gas} considers the effect of atmospheric conditions and substantial gas attenuation. The effect of rain attenuation is quantified by using way of A_r . The route loss is stricken by the space most of the transmitter and receiver in each equation. this is especially vital when it comes to making sure there is enough network insurance. Loss (PLdB) is calculated as follows:

$$PLdB = L_{LoS} + 10 \log_{10}(f_GHz) + 10 \log_{10}(d/1) + x \quad (9)$$

the second machine calculates the second one-course loss (PLdB) and integrates more variables:

Loss denotes a lack of line of sight. The word $10 \log_{10}(f_GHz)$ refers to the frequency of the sign in gigahertz (GHz). course loss due to distance between transmitter and receiver is represented through the expression $10 \log_{10}(d/1)$. 'x' is a variable that includes several affecting factors.

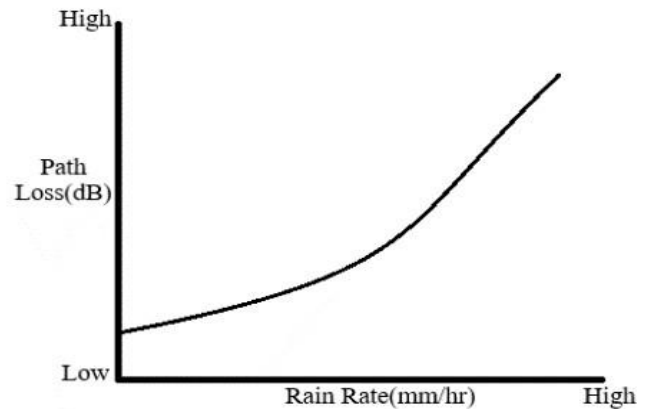


Fig. 3 Path Loss with respective Rain rate

A vital aspect of community layout and optimization, route loss estimation in wireless conversation networks is made feasible by using the approach of those formulae. the following are some key insights: Distance-related conduct The period of the route loss will grow with the distance most of the transmitter and receiver, this is taken into consideration in each equation. that is a crucial part of making sure of perfect network insurance.

The equation emphasizes that signal frequency (f_GHz) has an instantaneous impact on route loss. direction loss rises with frequency, emphasizing the need to pick out the proper frequency for a man or woman's verbal exchange desires.

Atmospheric and Environmental Considerations: Both models incorporate atmospheric conditions (A_{gas}) and rain attenuation (A_r), which are particularly significant in regions characterized by variable weather conditions. These elements can have a substantial impact on signal strength, especially in outdoor settings. Variable "x": In Formula, 'x' represents diverse environmental factors and influences. Taking these factors into consideration is essential when estimating path loss in real-world scenarios. Network Planning: These formulas are invaluable for network planning and design. They assist engineers in assessing signal strength at various distances and frequencies, facilitating network performance and coverage optimization.

Although it isn't specifically addressed in the above equations

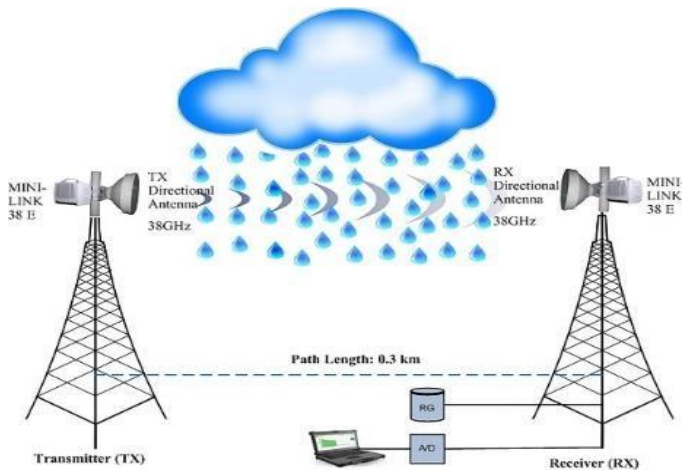


Fig.4 Path between two antennae

shadow fading—random variations in signal intensity brought on by ambient factors and interference—is an important factor to consider when designing wireless communication systems. The accuracy of path loss estimation can be improved by including shadow fading models.

4. RESULT

A. Discussion of Path Loss:

The results of a route loss versus rain rate plot often show the relationship between path loss and the amount of rainfall in a certain area. This link is essential in the realm of telecommunications, especially when creating wireless communication systems, because heavy rain may damage radio signals and reduce transmission quality as shown in Fig 5. The plot may go in a similar direction:

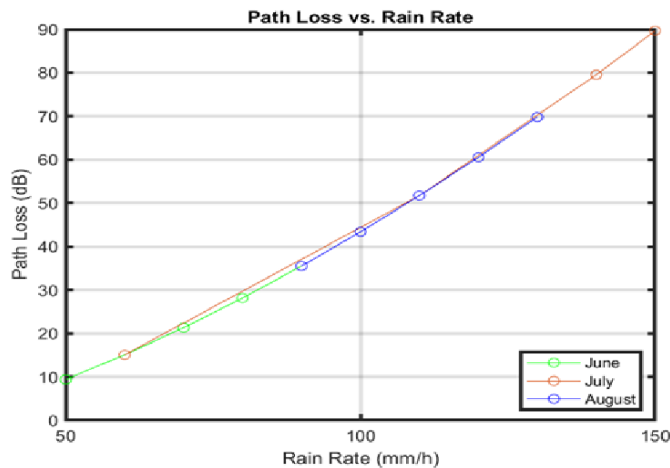


Fig. 5: Resultant of Path loss with rain rate

The x-axis in this graph represents the rate of precipitation n , which is frequently expressed in millimeters per hour (mm/hr) or decibels per millimeter (dB/mm). The path loss, which is often stated as a decibel (dB) number, is shown on the y-axis.

Important plot observations might be: Path Loss and Rain Rate: The plot will typically demonstrate the relationship between path loss and rain rate. This is because a greater path loss results from the attenuation, scattering, and absorption of radio signals by raindrops. The connection between path loss and rain rate is typically nonlinear. Small variations in the rain rate may at first have little impact on route loss, but as the rain rate increases, the route loss may quicken. Other factors including frequency, signal propagation characteristics, and the local environment might have an influence on the relationship between rain rate and route loss; as a result, the plot may exhibit changes in this area. Network engineers and planners employ these plots to sway their decisions on the creation and installation of wireless communication networks. To account for increased route loss during extreme rain events, they might need to use mitigation strategies such as power management, diversity tactics, or adaptive modulation. It is crucial to remember that the location, frequency range, and propagation model all affect how precisely the plot is shaped. The data required to create the graphic may have also been generated via simulations or field observations. Accurate route loss estimates and data are crucial for developing dependable and long-lasting wireless communication systems in regions subject to heavy rainfall.

B. Discussion of Rain fade slope:

Based totally on the input parameter A_r acquired from the ITU P.618 rain fade model, the characteristic computes the rain fade slope (denoted as rain fade slope(i)). This parameter is essential for determining how rain influences the attenuation of a verbal exchange link. The ITU P.618 version is a nicely hooked-up International Telecommunication Union (ITU) idea that calculates rain prompted attenuation for each satellite and terrestrial microwave communique connection at the same time as taking into account several meteorological and topographical situations. The predicted rain fade slope for a certain state of affairs is allocated to the i^{th} member of the 'rain_fade_slope' array on this code. The index 'i' suggests that several rain fade slopes are being computed, likely for diverse situations or frequency stages. Unfortunately, the unique approach or calculation used to derive the 'rain fade slope' from the ' A_r ' input is not provided within the code snippet. The real calculation should depend upon the specific implementation of the ITU P.618 version and the values of ' A_r ' getting used. The rain fade slope is a critical detail in satellite and microwave communication. It tracks how speedy the signal strength deteriorates at the same time as the rain rate increases. A steeper rain fade slope suggests that rain has an extra effect on the sign attenuation of the conversation hyperlink as shown below Fig 6. The results and their significance depend on the specific values of ' A_r ', the scenario or location under consideration (including factors like geographical location,

operating frequency, and atmospheric conditions), and the application of the ITU P.618 model. Engineers and communication system designers use these rain fade slope values to design robust communication links capable of withstanding varying levels of rain-induced attenuation.

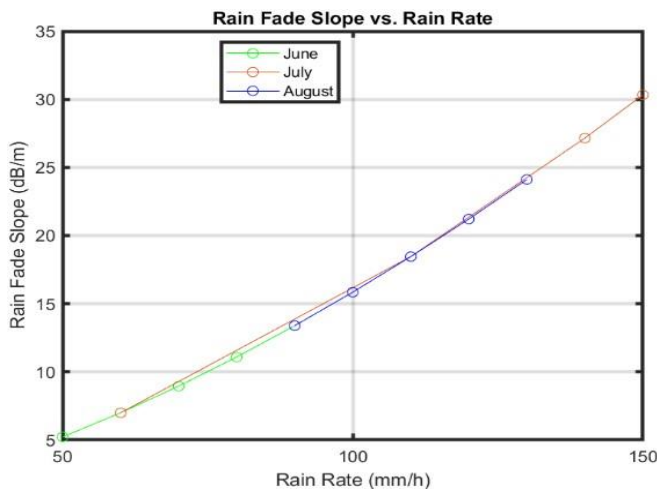


Fig. 6: Resultant of Rain fade slope with rain rate

More detailed analysis and interpretation of the results would require knowledge of the specific formula used to compute the rain fade slope from A_r . Additionally, the context in which this code is applied and the values of A_r and i would influence the practical implications of the results.

C. Discussion of Rain fade duration:

Understanding the connection between rain fade duration and rain rates is of paramount importance for ensuring the reliable operation of wireless communication systems in wet conditions. Continuous rainfall leads to short-lived signal disruptions, whereas more intense rain rates and longer rain fade durations result in extended communication failures. This relationship holds significant implications for the development of robust networks capable of withstanding heavy rainfall, impacting industries like satellite communications and telecommunications. Precise predictions of rain rates are indispensable for effectively managing and proactively addressing potential communication disruptions during heavy rainfall.

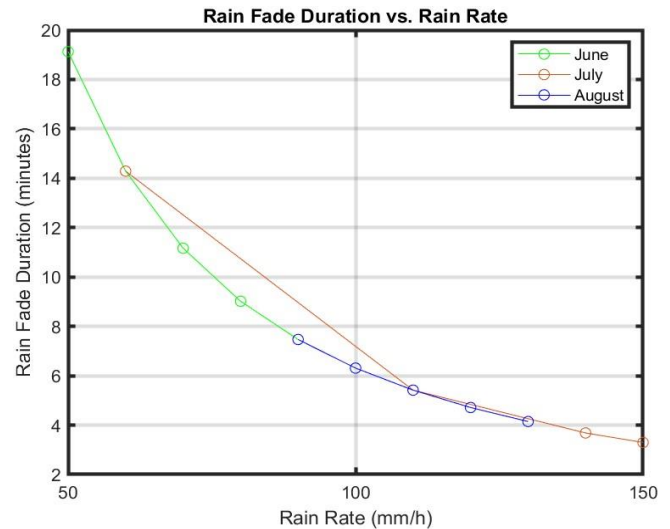


Fig. 7: Resultant of rain fades duration with respective rain rate

Nonlinear rainfall rates are likely to impact the duration of rain fade. Various factors, including environmental conditions, frequency range, and wireless communication technology, can influence the characteristics of these graphs. With increasing precipitation, signal outage periods may extend. Telecom professionals can utilize these graphical representations to assess the impact of rain-induced signal loss on communication networks. An understanding of rain fade duration is essential for designing systems with a substantial fade margin and implementing strategies like diversity reception or adaptive modulation to mitigate their effects as shown in fig 7. The specific shape of these graphs can be influenced by factors such as location, frequency range, and other system specific components. Professional engineers typically gather data for these representations through observations or models to inform decisions related to system deployment, development, and reliability in regions with heavy rainfall. Effective wireless communication, especially in wet environments, relies on a comprehensive understanding of the relationship between rain fade duration and rain rates. By examining this relationship, engineers can make informed decisions to minimize signal degradation and enhance coverage.

5. CONCLUSION

Rain fade becomes a serious problem when there is a lot of rainfall and satellite verbal exchange mechanisms are operating at high frequencies. Since the fade slope and period might vary greatly depending on the exact rain fade event, it may be difficult to predict and set limits for them. By using the ITU-R version, rainfall fade attenuation, fade slope, and

REFERENCES

1. NASA Earthdata Observatory System.
2. Budalal A.A. and Md. R. Islam, (2023). Path loss models for the outdoor environment—with a focus on rain attenuation impact on short-range millimeter-wave links, e-prime.
3. George R. MacCartney, Jr., Student Member, and Theodore S. Rappaport (2017). Rural Macrocell Path Loss Models for Millimeter Wave Wireless Communications, IEEE Journal on Selected Areas in Communications.
4. Andre H. and Nofriadi,(2017). International Journal of Engineering Science and Technology, analisis path loss spektrum frekuensi uhf untuk penyiaran tv terrestrial Kota Padang, Jurnal nasional teknik elektro.
5. Faruk N., Yinusa. A. Adediran, and Adeseko A. Ayeni, (2013). Error Bounds of Empirical Path Loss Models.
6. Kang T. and Seo J.,(2020). Practical Simplified Indoor Multiwall Path-Loss Model. h International Conference on Control, Automation and Systems.
7. Rui R. Paulo and Fernando J. Velez (2022). Impact of the Two-Slope Path Loss Model in the Service Quality of 4G and 5G Small Cells.
8. Maddikera, K.R., Kotamraju, S.K. & Kavya, K.C.S.(2023). Seasonal Rainfall Analysis of Vertically Pointing FMCW Micro Rain Radar. *SN COMPUT. SCI.* **4**, 559 <https://doi.org/10.1007/s42979-023-01987-8>
9. Maddikera, K. R., Kotamraju, S. K., Sri Kavya, K. C., & Gande T., B. G. (2022). Radar Reflectivity of Micro Rain Radar (MRR2) at 16.44180N, 80.620E of India. *International Journal of Integrated Engineering*, *14*(7),162185. <https://publisher.uthm.edu.my/ojs/index.php/ijie/article/view/10834>
10. Reddy M.K., J. C. Sekhar, Rao V.S., Md S.A Ansari, Yousef A.Baker El-Ebiary, Ramu J. and R. Manikandan (2013). Image Specular Highlight Removal using Generative Adversarial Network and Enhanced Grey Wolf Optimization Technique, *14*(6). [. http://dx.doi.org/10.14569/IJACSA.2023.0140668](http://dx.doi.org/10.14569/IJACSA.2023.0140668).
11. Maddikera, K. R., Kotamraju, S. K., Kavya, K. C. S., Kalyan, S. S. S., & TilakGande, B. G. Estimation of Melting Layer and Propagation Impairments Using Micro Rain Radar Data at Coastal Location of Andhra Pradesh.
12. Maddikera, L. R., & Maddikera, K. R. (2024). Investigating the Influence of Glass Fibres on Geopolymer Concrete's Mechanical Properties. In *Journal of Physics: . (2779(1),012068)*. IOP Publishing. DOI 10.1088/1742-6596/2779/1/012068.
13. Maddikera, K. R., Kotamraju, S. K., Kavya, K., & Gande, B. G. T.(2020). Zr relations of micro rain radar during cyclones, monsoon and clear sky conditions at coastal location of Andhra Pradesh. *Turk J Physiother Rehabil*, *32*(2).
14. Reddy, M. K., Priyanka, T., Nagendramma, M., Manasa, U., Manjuvani, M., & Pranitha, T. (2023). Revolutionizing Energy Efficiency with Roller-Assisted Power Hump Solutions. *Journal of Survey in Fisheries Sciences*, *10*(1S), 5562-5568. <https://doi.org/10.53555/sfs.v10i1S.1911>
15. <https://doi.org/10.52783/cana.v32.1648>
16. <http://hdl.handle.net/10603/601189>